Immunity, Vol. 22, 451–465, April, 2005, Copyright ©2005 by Elsevier Inc. DOI 10.1016/j.immuni.2005.01.018

Autoimmunity and Inflammation Due to a Gain-of-Function Mutation in Phospholipase Cγ2 that Specifically Increases External Ca^{2+} Entry

Philipp Yu,[1,2,*] Rainer Constien,[1,9] Neil Dear,[1,6] Matilda Katan,[3] Petra Hanke,[1,10] Tom D. Bunney,[3] Sandra Kunder,[4] Leticia Quintanilla-Martinez,[4] Ulrike Huffstadt,[1] Andreas Schröder,[1,11] Neil P. Jones,[3] Thomas Peters,[1] Helmut Fuchs,[5] Martin Hrabe de Angelis,[5] Michael Nehls,[1] Johannes Grosse,[1] Philipp Wabnitz,[1] Thomas P.H. Meyer,[1,12] Kei Yasuda,[2] Matthias Schiemann,[2,7] Christian Schneider-Fresenius,[1,13] Wolfgang Jagla,[1] Andreas Russ,[8] Andreas Popp,[1] Michelle Josephs,[3] Andreas Marquardt,[1] Jürgen Laufs,[1] Carolin Schmittwolf,[1] Hermann Wagner,[2] Klaus Pfeffer,[2,14] and Geert C. Mudde[1,15]

[1]Ingenium Pharmaceuticals AG
Fraunhoferstrasse 13
82152 Martinsried, Munich
Germany

[2]Institute of Medical Microbiology, Immunology and Hygiene
Technical University Munich
Clinic Rechts der Isar
Trogerstrasse 4a
81675 Munich
Germany

[3]Cancer Research UK Centre for Cell and Molecular Biology
Chester Beatty Laboratories
The Institute of Cancer Research
Fulham Road
London SW3 6JB
United Kingdom

[4]Institute of Pathology

[5]Institute of Experimental Genetics
GSF-National Research Center for Environment and Health
Ingolstädter Landstrasse 1
85764 Neuherberg
Germany

[6]Mary Lyon Centre
Medical Research Council
Harwell, Didcot OX11 0RD
United Kingdom

[7]Clinical Cooperation Group Vaccinology
GSF-National Research Center for Environment and Health and
Technical University Munich
Trogerstrasse 4b
81675 Munich
Germany

[8]Genetics Unit
Department of Biochemistry
University of Oxford
South Parks Road
Oxford OX1 3QU
United Kingdom

*Correspondence: philipp.yu@lrz.tum.de

[9]Present address: Alnylam Europe AG, Fritz-Hornschuch-Strasse 9, 95326 Kulmbach, Germany.

Summary

The identification of specific genetic loci that contribute to inflammatory and autoimmune diseases has proved difficult due to the contribution of multiple interacting genes, the inherent genetic heterogeneity present in human populations, and a lack of new mouse mutants. By using N-ethyl-N-nitrosourea (ENU) mutagenesis to discover new immune regulators, we identified a point mutation in the murine phospholipase Cg2 (*Plcg2*) gene that leads to severe spontaneous inflammation and autoimmunity. The disease is composed of an autoimmune component mediated by autoantibody immune complexes and B and T cell independent inflammation. The underlying mechanism is a gain-of-function mutation in *Plcg2*, which leads to hyperreactive external calcium entry in B cells and expansion of innate inflammatory cells. This mutant identifies Plcg2 as a key regulator in an autoimmune and inflammatory disease mediated by B cells and non-B, non-T haematopoietic cells and emphasizes that by distinct genetic modulation, a single point mutation can lead to a complex immunological phenotype.

Introduction

Spontaneous inflammation and autoimmunity occur together in diseases such as systemic lupus erythematosus (SLE), rheumatoid arthritis, and Wegener's granulomatosis (WG) (Sack and Fye, 2001). Indeed, the association is so tight that it is not known whether an unrestrained inflammatory response or an inappropriate autoimmune response to self-antigen or both initiate the diseases. Molecular mechanisms involved are further obscured by the complex genetics underlying this group of diseases that make identification of key regulatory genes difficult (Roberton and Vyse, 2000; Ueda et al., 2003; Wollheim et al., 2003).

To identify genetic alterations in genes involved in autoimmunity or inflammation, we employed large-scale ENU mutagenesis in the mouse together with clinical screening for relevant phenotypes. Mice with profound immunological alterations were identified, and positional cloning of the mutations was performed (Hrabe de Angelis et al., 2000; Nelms and Goodnow, 2001). The

[10]Present address: Roche Diagnostics GmbH, Nonnenwald 2, 82372 Penzberg, Germany.

[11]Present address: Baxter Germany GmbH, Im Breitspiel 13, 69126 Heidelberg, Germany.

[12]Present address: Blood Donor Service of the Bavarian Red Cross, Herzog-Heinrich-Strasse 4, 80336 Munich, Germany.

[13]Present address: Lilly Deutschland GmbH, Saalburgstrasse 153, 61350 Bad Homburg, Germany.

[14]Present address: Institute of Medical Microbiology, Heinrich-Heine-Universität Düsseldorf, Universitätsstrasse 1, 40225 Düsseldorf, Germany.

[15]Present address: IGENEON AG, Brunner Strasse 69, 1230 Vienna, Austria.

advantage of this forward genetics approach is the immediate association of gene and phenotype without previous assumptions about physiological gene function. Importantly, this strategy allows the identification of hypermorphic mutations, resulting in insights that could not be readily obtained with the conventional backward genetics approach, i.e. gene knockout, now dominantly employed in mouse genetics (Nathan, 2002).

From a genetic point of view, it is important to note that all human autoimmune inflammatory diseases seem to be multigenic, whereas evidence for complex genetic interactions has been presented for only two out of 40 gene knockout models of inflammation (Nathan, 2002). Only the IL-1Rα and FcγRIIb loss-of-function phenotypes are modulated in different genetic backgrounds (Bolland and Ravetch, 2000; Horai et al., 2000), making them more relevant models for human diseases.

Like other signaling molecules, PLCG2 seems to be integrated into the complex regulation of the immune system. It is a member of the phosphoinositide-specific phospholipase C (PI-PLC) family, is highly expressed, and is required for function of haematopoietic cells, including B cells, NK cells, mast cells, macrophages, and platelets (Hiller and Sundler, 2002; Kurosaki et al., 2000; Wang et al., 2000; Wen et al., 2002). In T cells, however, the other member of the PLCγ subfamily, PLCγ1, has a major functional role. Despite the recognition of the PI-PLC family as key enzymes in signal transduction for nearly three decades (Rhee, 2001), the complex regulatory mechanisms of PLCγ isoforms have been appreciated only recently (Patterson et al., 2002; Ye et al., 2002). Generally, PLCγ isoforms are localized in the cytoplasm but are recruited to the membrane upon receptor activation where further protein-protein and protein-lipid interactions, together with tyrosine phosphorylation, contribute to their activation. For PLCγ2, such a signaling mechanism is best defined in B cell responses (Kurosaki et al., 2000; Marshall et al., 2000). Briefly, the stimulation of the B cell receptor (BCR) and other receptors regulates PLCγ2 through a set of protein tyrosine kinases (Lyn, Syk, and Btk) and inositol-lipid-kinases (PI-3K) that generally contribute to activation, whereas phosphatases acting on the same substrates (tyrosine phosphatase SHP-1 and inositol-lipid phosphatase SHIP) have an inhibitory impact (Coggeshall et al., 2002). Membrane interactions of the assembled BCR signalosome are stabilized by production of phosphatidylinositol 3,4,5-trisphosphate (PIP_3) that binds to pleckstrin homology (PH) domains of Btk and PLCγ2 itself. The catalytic domain of PLCγ2 also has to interact with the membrane to access and hydrolyze the substrate phosphatidylinositol 4,5-bisphosphate (PIP_2) to generate diacylglycerol (DAG) and inositol 1,4,5-trisphosphate (IP_3) (Hurley and Grobler, 1997). In immune cells, as in other cell types, the production of these secondary messengers leads to activation of DAG targets (e.g., protein kinase C) and an increase in intracellular Ca^{2+}, which has been recognized as crucial in mediating a variety of cellular responses (Rhee, 2001; Wilde and Watson, 2001). The tight connection between PLCγ activity and Ca^{2+} increase in the cytoplasm has recently been emphasized by the discovery of a novel mechanism by which PLCγ can mediate external Ca^{2+} entry independent of its catalytic activity, probably through protein-protein interactions (Patterson et al., 2002; Putney, 2002; Putney et al., 2001; van Rossum et al., 2005). Despite the extensive experimental evidence supporting that activation of PLCγ and, particularly, the downstream Ca^{2+} flux are important signaling events in cellular activation or apoptosis, relatively limited advances have been made to assess its potential role in disease.

Here, we identify and characterize a gain-of–function mutation in Plcg2 and show the consequences of enhanced Plcγ2 signaling in vivo. On the cellular level, augmented external Ca^{2+} entry is shown. Deregulation of different components of the immune system, namely B cells and cells of the innate immune system, underlie autoimmune and inflammatory symptoms in mutant mouse strains. Crossing of the mice to a different genetic background and to lymphocyte-deficient mice suggest different independent mechanisms of pathology induced by the *Plcg2* mutation.

Results

Differential Pathology of *Plcg2*^{Ali5} Mice Depends on Genetic Background and Gene Dosage Effects

From a single female of the first generation of offspring of ENU-treated C3HeB/FeJ (C3H) mice, the mouse line Ali5 (*A*bnormal *li*mb 5) was established on the basis of dominant inheritance of spontaneous swollen and inflamed paws. In addition, 50% of the offspring displayed an abnormally high ratio of T cells versus mature B cells (Figure 2A). Maintaining the line on a wild-type (wt) C3H background for more than ten generations demonstrated that the inheritance of the phenotype was autosomal dominant and coincided with male infertility (P.Y., N.D., U.H., S.K., L.Q.-M., unpublished data). In C3H mice, the penetrance was 100% for the abnormal T:B cell ratio but only 60%–80% for the swollen paw phenotype.

The nonconservative amino acid exchange in Plcγ2^{Ali5} results in severe and complex pathology in vivo (Figures 1A–1U and overview in Table 1). C3H-inbred *Plcg2*$^{Ali5/+}$ mice have normal paws at birth but gradually develop swollen and deformed footpads (Figures 1A–1F). Male mice were affected earlier than female mice (2 months cf. 8–10 months). Initially, dermatitis developed in the superficial layers of the skin of the paws and ears (Figures 1E–1H). The infiltrate included granulocytes, macrophages, lymphocytes, mast cells, and eosinophils (data not shown). This chronic inflammation gradually affected the bone, resulting in severe arthritis of the small joints of the paws and missing phalanges (Figures 1C–1F).

In contrast, the heterozygous C57BL/6J × C3HeB/FeJ (B6C3) mice (N_2 and N_3 backcross generation) had no inflammation, neither macroscopically nor histologically (Figure 1I and data not shown). However, three out of ten hybrid *Plcg2*$^{Ali5/+}$ mice showed signs of glomerulonephritis (see below). Intercrossing of the N_1 or N_2 *Plcg2*$^{Ali5/+}$ mice yielded offspring homozygous for the mutation. ~90% of homozygotes suffered from severe inflammation of the paws, but unlike heterozygous C3H

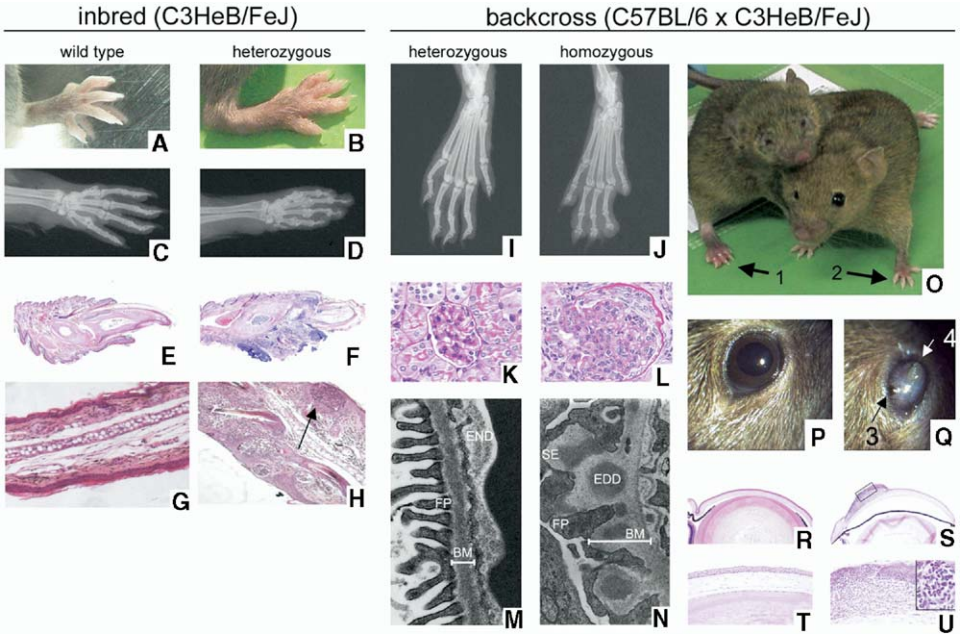

Figure 1. Pathology of Ali5 Mice

(A–H) Inbred C3H background. (A) Paw of a wild-type (wt) mouse (aged 62 days). (B) Swollen paw of a Plcg2$^{+/Ali5}$ littermate. (C) Radiography of a paw of a wt mouse (aged 405 days). (D) Plcg2$^{+/Ali5}$-affected littermate show bone destruction and loss of bone density, enlarged soft tissue shadow, and exostosis around the interphalangeal joints. (E) Histological analysis of the phalanges. HE staining of middle and distal phalanx of control animal (aged 405 days, 40×). (F) Inflamed phalanx of a Plcg2$^{+/Ali5}$ mouse (aged 73 days). (G) HE staining of the ear of a wt mouse (aged 90 days). (H) Ear of the *Plcg2*$^{Ali5/+}$ littermate (100×; arrow shows circumscriptive infiltration).

(I–U) Hybrid B6C3 *Plcg2*$^{Ali5/+}$ and *Plcg2*$^{Ali5/Ali5}$ mice. (I) Radiographs of paw of a *Plcg2*$^{Ali5/+}$ mouse (aged 77 days) showing no alterations. (J) *Plcg2*$^{Ali5/Ali5}$ littermates show similar paw phenotype to inbred *Plcg2*$^{Ali5/+}$ mice (see [D]). (K) Histology of the kidney (PAS stain, 400×) shows a normal glomerulum of a *Plcg2*$^{Ali5/+}$ mouse. (L) *Plcg2*$^{Ali5/Ali5}$ mice with intracapillary and extracapillary proliferative glomerulonephritis. (M) Electron microscopy of a normal kidney (Abbreviations: FP, foot processes of the podocytes; BM, base membrane; END, endothelium). (N) A *Plcg2*$^{Ali5/Ali5}$ mouse showing fusion of FP and electron dense deposits (EDD) in the subepithelial region (SR) of the BA. (O) *Plcg2*$^{Ali5/+}$ mouse (right) with normal eyes and paws (arrow 2) and a *Plcg2*$^{Ali5/Ali5}$ littermate (left) with eye deformations and crippled paws (arrow 1). (P) Comparison of a normal eye of a heterozygous mouse and (Q) an affected eye of a *Plcg2*$^{Ali5/Ali5}$ mouse, which shows proliferation of cells in the epithelium (arrow 4) and thinning of the sclera (arrow 3). (R and T) The *Plcg2*$^{Ali5/+}$ mouse has a normal structure of the cornea (40×, 160×). (S) HE section of a *Plcg2*$^{Ali5/Ali5}$ mouse with keratitis (40×). (U) Higher magnification shows destruction of the different layers of the corneal epithelium with keratinization (160×). The inflammatory infiltrate is composed of neutrophil granulocytes, eosinophils and lymphocytes (insert, 640×).

mice, they developed severe keratitis (nine out of ten mice) and proliferative intra- and extracapillary glomerulonephritis (eight out of eight mice; Figures 1K–1N and 1O–1U). The different phenotypes arising from the various combinations between genetic background and gene dosage of the mutant allele suggest that genetic modifiers modulate the penetrance and the quality of the *Plcg2*^{Ali5}-induced pathology.

Identification of Mutant *Plcg2*^{Ali5} by Positional Cloning

Mice that carry the *Plcg2*^{Ali5} allele in a hybrid B6C3 background displayed no paw abnormalities and showed a reduced but nevertheless elevated ratio of T cells versus mature B cells (Table 1 and Figure 2A). This altered ratio was fully penetrant and therefore used as a marker for positional cloning purposes. Genetic mapping narrowed the mutation to a 1.3 Mb region on chromosome 8 (Figures 2B and 2C). Sequencing of all exons of all five genes in this region identified a single A-G exchange in exon 27 of the *Plcg2* gene (Figure 2D). The mutation was present in all affected mice (n > 300). The mutation results in a single amino acid substitution of aspartic acid with glycine at position 993 (D993G). This aspartic acid is conserved in all PLC isoforms (Figure 2E). We have named this allele *Plcg2*^{Ali5}. The mutation was maintained in a C3H background by breeding heterozygous Plcg2$^{Ali5/+}$ mice to wt C3H animals for more than ten generations, such that statistically 99.9% of the genome of the original F1 founder genome has been replaced. During this process, the original phenotype was stable and the phenotype strictly segregates with the *Plcg2* genotype in all affected mice tested (>300).

The aspartic acid residue mutated in Plcγ2^{Ali5} is located within the region of the catalytic domain described as a "ridge" surrounding the active site opening of Plcγ2 that has been suggested to exert an inhibitory impact on PLC activity by preventing extensive membrane interactions (Ellis et al., 1998) (Figure 3A). It is interesting to note that the inside of eukaryotic plasma membranes is negatively charged. So the loss of a

Table 1. Phenotype Overview

	C3HeB/FeJ		C3HeB/FeJ x C57BL/6J		
Genotype	Plcg2$^{+/Ali5}$	Plcg2$^{+/+}$	Plcg2$^{Ali5/Ali5}$	Plcg2$^{+/Ali5}$	Plcg2$^{+/+}$
Phenotype					
Ratio T cell/mat. B2 cell[a]	13.5	1.3	5.2	3	2.1
Paw inflammation	Yes	No	Yes	No	No
Autoantibodies	No	No	Yes (66%)	Yes (28%)	No
Glomerulonephritis	No	No	Yes (100%)[b]	Yes (30%)[c]	No
Growth retardation	No	No	Yes	No	No
Keratitis	No	No	Yes	No	No

Summary of phenotypes using Ali5 and littermate controls in C3HeB/FeJ and hybrid C3HeB/FeJ × C57BL/6J N_2 or N_3 genetic background.
[a] In peripheral blood.
[b] Eight out of eight tested.
[c] Three out of ten tested.

negative charge by the D993G mutation in this important region of the molecule might reduce repulsion of Plcγ2^{Ali5} from the membrane.

The Point Mutation in Plcg2^{Ali5} Is Likely to Increase the Extent of Membrane Interactions Rather than the Properties of the Phospholipase Active Site

To assess Plcg2^{Ali5} function in a signaling context, we focused on well-characterized responses of B cells. In purified B cells from C3H *Plcg2$^{Ali5/+}$* mice, normal *Plcg2^{Ali5}* mRNA expression was detected (Figure 3B). However, moderately reduced expression of Plcg2^{Ali5} protein was seen in both C3H and C3B6 mice (Figure 3C).

Our initial data using DNA arrays to analyze purified B cells from *Plcg2$^{Ali5/+}$* C3H mice and wt littermates revealed differences in gene expression (data not shown). Interestingly, the upregulated mRNAs included those for S100a9 and S100a6, but not Plcγ2, Igα, and Map2K (Figure 3B). The S100 family of molecules is believed to function through direct calcium binding and is also implied in inflammation (Roth et al., 2003; Ryckman et al., 2003); this further supports the importance and complexity of changes in calcium responses.

Analysis of Plcγ2 basal activity using purified recombinant protein in mixed micelles in vitro, bypassing requirements for membrane interactions, showed a slightly, but not significantly, elevated activity of the mutant (Figure 3D). This is consistent with the position of this mutation at the membrane interaction surface and previous findings that mutations within this region in PLCδ1 affected PLC function by increasing membrane interactions rather than changing properties of the active site.

To examine this further, we performed membrane localization studies of wt and mutant Plcγ2 expressed in the WEHI-231 B cell line. Before stimulation, neither wt nor mutant Plcγ2 can be detected at the cytoplasmic membrane. Addition of anti-IgM Ab induces the recruitment of Plcγ2 to the membrane in comparable amounts. However, at later timepoints (15 min), this recruitment is noticeably more prominent for Plcγ2^{Ali5} (Figure 3E). Because the hydrophobic ridge is one of several domains (e.g., PH and SH2 domains) that contribute to membrane interactions, its importance in regulating Plcγ2 functions can be exerted earlier through subtle changes in the enzyme positioning, which could not be simply assessed by monitoring membrane interactions. It is, however, possible that at later time points, in the absence of other interactions, mutations in the hydrophobic ridge prolong membrane association.

In summary, these results imply that the Ali5 mutation in *Plcg2* does not result in an overexpression of *Plcg2* in vivo and has no effect on basal phospholipase enzymatic activity of Plcγ2 in vitro, rather, the mutation changes its ability to interact and remain at the cytoplasmic membrane. This in turn may enhance or prolong its activity postactivation.

Plcγ2^{Ali5} Induces Increased and Sustained External Calcium Entry in B Cells

To examine Ca^{2+} mobilization after anti-IgM stimulation, we first confirmed that B cells from inbred C3H *Plcg2$^{+/Ali5}$* and *Plcg2$^{+/+}$* mice had comparable levels of IgM surface expression (Figure 4A). *Plcg2$^{+/Ali5}$* B cells responded with a higher initial peak and sustained Ca^{2+} levels when a complete anti-IgM antibody was used to stimulate the BCR (Figure 4A, 1 versus 2). This Ca^{2+} response in Ali5 is similar to responses in B cells lacking inhibitory signals normally generated by coligation of FcγRIIb (Ravetch and Bolland, 2001). The absence of SHIP activation under such circumstances results in higher PIP_3 levels, which stabilize Btk and Plcγ2 membrane interactions, resulting in sustained IP_3 production and Ca^{2+} responses (Scharenberg and Kinet, 1998). Indeed, the removal of this inhibitory signal using a $F(ab')_2$-anti-IgM fragment reduced differences between the mutant and wt Plcγ2 protein, but a higher sustained Ca^{2+} response was still observed in mutant B cells (Figure 4A, 3 versus 4). This suggests that the Ali5 mutation might contribute to stabilization of membrane complexes, thus substituting for PIP_3 binding.

To confirm that the changes in Ca^{2+} signaling are the result of the mutation in *Plcg2*, the wt and mutant proteins were expressed in primary LPS-activated wt B cells by retroviral transfection of *Plcg2* cDNA expression constructs. Both the wt and mutant Plcγ2 proteins induced an elevated Ca^{2+} baseline and stronger Ca^{2+} signal upon anti-IgM stimulation (Figure 4B, 3 and 4) compared to the endogenous *Plcg2* (Figure 3B, 1 and 2). Expression of *Plcg2^{Ali5}* in the B cells resulted in

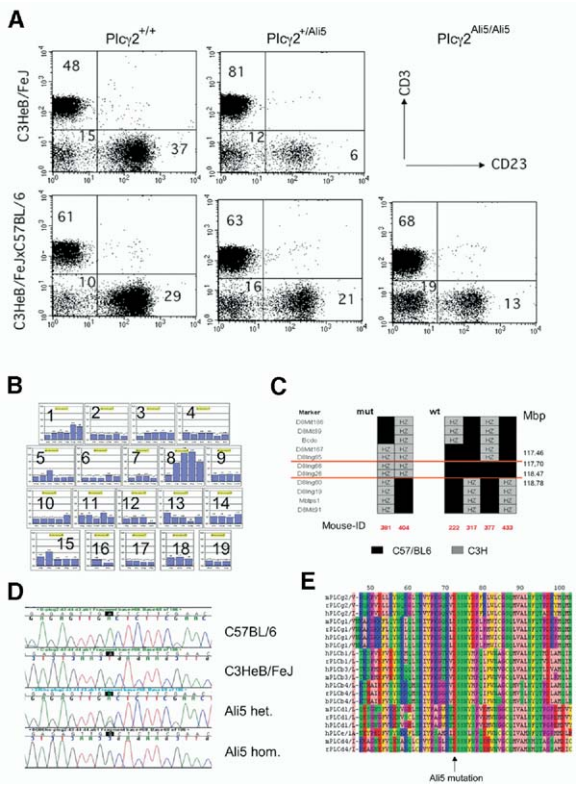

Figure 2. Identification of a Point Mutation in *Plcg2* in Ali5 Mice

(A) Flow cytometric analysis of peripheral blood of Ali5 mice. Numbers indicate the percentage of gated populations of T cell (anti-CD3) versus mature B2 cell (anti-CD23) lymphocyte populations in peripheral blood. This staining was used as the phenotypic screen for the positional cloning.

(B) Identification of a point mutation in the *Plcg2* gene. One step chromosomal mapping by determination of the SNP allele frequency of unaffected mice of the Ali5 line. ~90 SNPs polymorphic between C3HeB/FeJ and C57BL/6J strains, which are equally distributed over the 19 autosomal mouse chromosomes, were used,. SNP allele frequency was measured by using Pyrosequencing technology. The Ali5-negative DNA pool analysis showed increased proportions of BL/6 alleles on chromosome 8. Statistically, one expects an average BL/6 to C3H ratio of 3 at an unlinked marker in N_2 animals. The ratio is much higher (maximum of 13) on chromosome 8.

(C) Fine mapping using informative Ali5 mice. The proximal border is defined by flanking marker D8Ing65 of mouse ID 377, whereas the distal flanking marker DIng60 is informative in three mice: 404, 317, and 433. The position of the two internal and two flanking marker is given in Mb with respect to the mouse genome assembly MGSCv3.

(D) Sequence of murine *Plcg2* from wt, heterozygous *Plcg2*$^{Ali5/+}$ (Ali5 het.), and homozygous *Plcg2*$^{Ali5/Ali5}$ mice (Ali5 hom.) revealed an A→G mutation in Ali5. The figure shows the sequence chromatogram from exon 27 around the mutation site. Where C3H and BL/6 carry an A at the respective position, Ali5 heterozygous mice show a G/A double peak, and Ali5 homozygous mice carry only a G.

(E) A multiple sequence alignment of part of the Y catalytic domain of different PLC protein family members from three different species (mouse, rat, and human) showing the high level of conservation between the three species and the location of the mutation (arrow at the D for aspartic acid).

downregulation of IgM surface expression in vitro (Figure 4B). Nevertheless, cells with Plcg2^{Ali5} responded to F(ab′)$_2$-anti IgM with a more sustained Ca^{2+} elevation than those with wt Plcg2 (Figure 4B, 3 and 4). This suggests that Plcγ2^{Ali5} activity underlies the changes in Ca^{2+} responses.

In order to further examine the pathway of Ca^{2+} influx, we withdrew exogenous Ca^{2+} and added EGTA. This led to a complete inhibition of the increased Ca^{2+} response (Figure 3C, compare 1 and 2 in the top panel with 1 and 2 in the bottom panel), suggesting that the Ca^{2+} efflux from the internal stores to the cytoplasm is not affected by the D993G mutation, whereas the plasma membrane channel-mediated Ca^{2+} entry from the outside is dramatically elevated (Figures 4C–4E). Thapsigargin-mediated depletion of internal Ca^{2+} stores and the increase of cytoplasmic Ca^{2+} lead to opening of external Ca^{2+} plasma channels, by an unknown mechanism, independent of Plcγ2 function (Putney, 2002; Putney et al., 2001). Both internal and external thapsigargin-activated Ca^{2+} fluxes were not altered in Ali5 B cells (Figure 4C, compare 3 and 4 in the top panel with 3 and 4 in the bottom panel). This proves that changes in external Ca^{2+} entry are dependent on physiological BCR activation of Plcγ2, but not by a mere increase of the cytoplasmic Ca^{2+} concentration. Heterozygous Ali5 B cells on a hybrid B6C3 background respond similarly to mutant C3H B cells (Figure 4C) after BCR and thapsigargin stimulation (Figures 4D and 4E).

We also compared the Ca^{2+} flux of B cells from wt, heterozygous, and homozygous *Plcg2*^{Ali5} mice by using the Ca^{2+} fluorophore Indo-1, which is less prone to loading artefacts. Stimulation with complete anti-IgM leads to enhanced and sustained cytoplasmic Ca^{2+} concentrations in both heterozygous and homozygous B cells (Figure 4E). In cells from wt mice, this response could be completely inhibited by the addition of 0.2 μM of the phospholipase C inhibitor U73122 (Figure 4E, top, 4 and 5) (Taylor and Broad, 1998). However, it is notable that while being strongly inhibited, mutant cells still displayed a low but detectable Ca^{2+} increase (Figure 4E, bottom).

In contrast to changes in B cell calcium responses, Ali5 T cells did not show an enhanced Ca^{2+} response after TCR stimulation (Figure 4A, 5 and 6). This is in line with a predominant expression of *Plcg1* rather than *Plcg2* in these cells.

In addition to changes in calcium concentrations, the production of IP_3 was also monitored and found to be increased in both B cells from Ali5 mice and WEHI-231 cells expressing mutated *Plcg2*. For WEHI/Plcg2^{wt}, the basal level was 1.5 ± 0. 1 (pmol/assay) and increased after stimulation with IgM to 1.8 ± 0.2 after 30 s and to 2.2 ± 0.2 after 60 s. For WEHI/Plcg2^{Ali5}, the basal level was 1.5 ± 0.1 and increased after stimulation to 3.1 ± 0.4 after 30 s and to 4.2 ± 0.4 after 60 s. IP_3 returned to the basal level after 240 s. In B cells from the wt mice, the basal level was 0.19 ± 0.03 and increased after stimulation with IgM to 2.3 ± 0.2 after 30 s and to 6.2 ± 0.5 after 60 s. For Ali5 mice, the basal level was 0.2 ± 0.03 and increased after stimulation with IgM to 2.6 ± 0.1 after 30 s and to 10.1 ± 0.7 after 60 s.

Taken together, these results imply that the Ali5 mu-

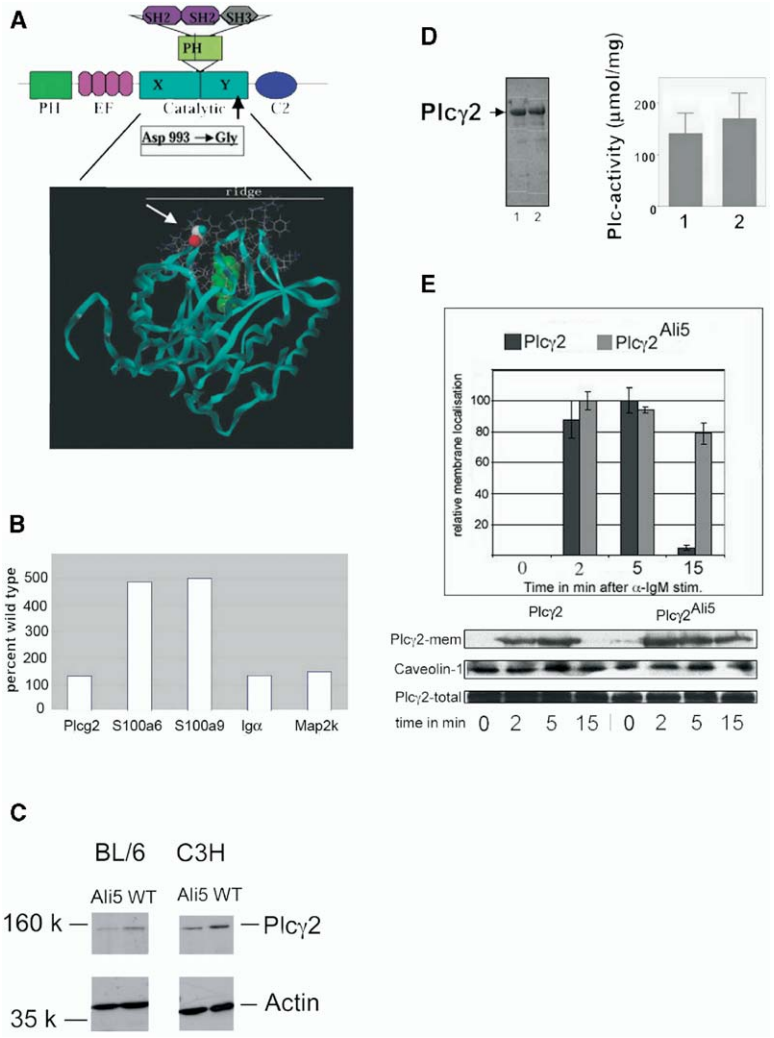

Figure 3. The Plcγ2^{Ali5} Mutation, *Plcg2* Expression, In Vitro Enzymatic Activity of Mutant Plcγ2, and Membrane Localization of Mutant Plcγ2

(A) Domain structure of Plcγ2 and ribbon diagram model on the basis of the rat Plcδ1 crystal structure (Essen et al., 1996) of the catalytic domains (X and Y) of murine Plcγ2. The three loops that surround the active center, which contains the substrate (green), extend toward the inner side of the cytoplasmic membrane. They form a ridge that points toward the membrane. The position of the asp^{993} to gly^{993} mutation is depicted by the spheres (arrow). Abbreviations: PH, pleckstrin homology domain; EF, EF-hand domain; SH2/SH3, src homology domain 2 and 3; and C2, C_2 domain.

(B) Quantitative PCR analysis of *Plcg2* expression in purified B cells from inbred heterozygous *Plcg2*$^{Ali5/+}$ C3H mice and wt littermates. *Plcg2* and two control genes (Iga and Map2k) were expressed at normal levels, and the genes S100a9 and S100a6, previously identified as dysregulated in a DNA chip experiment (data not shown), were confirmed as upregulated.

(C) Plcγ2 protein expression in purified B cells from hybrid B6C3 and C3H *Plcg2*$^{Ali5/+}$ mice. Plcγ2-specific Western blot (top) and actin-loading control (bottom) are shown.

(D) Enzymatic activity of recombinant Plcγ2 enzyme. The wt Plcγ2 (1) and Plcγ2^{Ali5} (2) were purified (left) and subsequently used for determination of basal-specific activity toward PIP_2 substrate in a micelle in vitro system (right). Km values obtained by using the same assay were 129 ± 14 μM for the wt and 131 ± 10 μM for the Ali5 mutant. Error bars represent the mean ± SD.

(E) Membrane localization of Plcγ2 after anti-IgM stimulation. WEHI-231 cells transfected with retrovirale vectors containing wt (dark bars) and mutant Plcγ2 (light bars) were stimulated, and the membrane localized Plcγ2 was detected by Western blot. Caveolin-1 and total Plcγ2 are shown as membrane fraction and protein expression controls, respectively. Error bars represent the mean ± SD.

tation in *Plcg2* represents a gain-of-function hypermorphic mutation that is active in vivo. It induces a higher and sustained Ca^{2+} flux into the cytoplasm, probably by influencing the external Ca^{2+} entry through plasma membrane channels in response to BCR activation.

Expansion of Innate Immune Cells in the Bone Marrow of *Plcg2*^{Ali5} Mice and Disease Transfer via Bone Marrow Transplantation

Both inflammatory cells of the innate and the cells of the adaptive immune system arise from bone marrow and share similar signaling pathways that require the presence of Plcγ2 (Bourette et al., 1997; Wang et al., 2000). Because histology of the affected organs showed increased numbers of granulocytes in infiltrates, we analyzed cells of the bone marrow where granulocytes arise. We identified similar total numbers of bone marrow cells in mutant and wt mice (wt-B6C3 = 2.9 × 10^7, n = 4; *Plcg2*$^{Ali5/+}$ B6C3 = 3.1 × 10^7, n = 4; *Plcg2*$^{Ali5/Ali5}$ B6C3 = 2.7 × 10^7, n = 3; wt-C3 = 1.7 × 10^7, n = 4; and *Plcg2*$^{Ali5/+}$ C3H = 1.8 × 10^7, n = 4). However, an increased ratio of granulocyte/macrophage to lymphocyte precursors was observed in Ali5 mice. The *Plcg2*$^{Ali5/Ali5}$ B6C3 hybrid mice had a 10-fold increase and inbred C3H *Plcg2*$^{Ali5/+}$ mice a 2-fold increase compared to *Plcg2*$^{+/+}$ littermates (Figure 5A). Additionally, the Gr1^{low}/CD11b-positive macrophage precursor population was increased by about 50% in inbred *Plcg2*$^{+/Ali5}$ and *Plcg2*$^{Ali5/Ali5}$ mice (Figure 5A). In order to further examine the role of bone marrow-derived haematopoietic cells, we transplanted bone marrow cells from a severely affected B6C3 *Plcg2*$^{Ali5/Ali5}$ mouse into wt mice. Two out of ten mice developed swollen and inflamed paws 4 weeks after the transfer, indicating that haematopoietic cells can transfer the disease (Figure 5B).

To answer the question about whether transferred lymphocytes develop normally, we analyzed the ratio of repopulating B versus T cells. Upon transfer to irradiated wt recipients, the ratio of B cells to T cells was four for wt (n = 2), but consistently below one for transfer of homoyzgous Ali5 bone marrow (n = 9). This demonstrates that the reduced B cell number is an effect intrinsic to cells derived from transferred bone marrow. Whether the effect is intrinsic to B cells or dependent

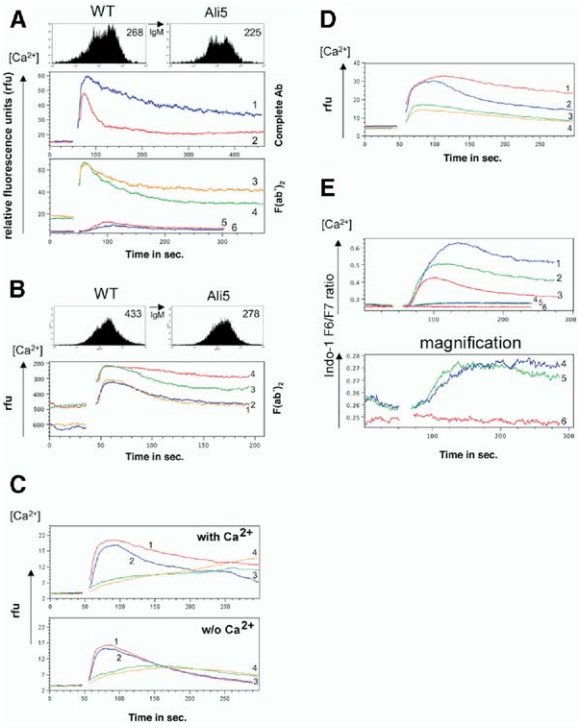

Figure 4. Ca^{2+} Mobilization in B Cells

(A) Ex vivo B cell stimulation of cells from inbred C3H *Plcg2*$^{Ali5/+}$ and wt littermates. Histograms show IgM expression of purified B cells (values are mean fluorescence). Spleen cells were loaded with Fluo-3 and stimulated by anti-IgM (either complete anti-IgM or the anti-IgM $F(ab')_2$ fragment) or anti-TCR Ab, and the fluorescence was measured by flow cytometry in relative fluorescence units (rfu). Ali5 B cells, complete Ab (1); wt B cells, complete Ab (2); Ali5 B cells, $F(ab')_2$ (3); wt B cells, $F(ab')_2$ (4); wt T cells, anti-TCR (5); and Ali5 T cells, anti-TCR (6).

(B) In vitro Ca^{2+} mobilization in primary B cells infected with wt and mutant *Plcg2* in MIGR1 retroviral vectors (which also contain IRES-GFP). Histograms show IgM expression of cells. Cells were loaded with Fura-Red, counterstained with B220, and stimulated with anti-IgM $F(ab')_2$. GFP-negative cells are not transfected by the GFP-containing retrovirus and serve as negative control (1,2). Note that Fura-Red has an inverse correlation to Ca^{2+} concentration, as higher Ca^{2+} results in lower fluorescence emission. MIGR1^{Ali5}-GFP^{negative} (1); MIGR1^{WT}-GFP^{negative} (2); MIGR1^{WT}-GFP^{positive} (3); and MIGR1^{Ali5}-GFP^{positive} (4).

(C) Internal and external Ca^{2+} flux in primary B cells. Ex vivo B cell stimulation of cells from inbred C3H *Plcg2*$^{Ali5/+}$ mice or wt littermates by anti-IgM-$F(ab')_2$ and thapsigargin. Spleen cells were loaded with Fluo-3 as described and activated in Ca^{2+} containing buffer (top) or without Ca^{2+} but containing EGTA (bottom). Ali5 B cells, $F(ab')_2$ (1); wt B cells, $F(ab')_2$ (2); Ali5 B cells, thapsigargin (3); and wt B cells, thapsigargin (4).

(D) Ca^{2+} influx in primary B cells from hybrid B6C3 heterozygous Plcg2$^{+/Ali5}$ and wt littermates by anti-IgM-$F(ab')_2$ and thapsigargin. Spleen cells were loaded with Fluo-3 as described and activated in Ca^{2+} containing buffer. Ali5 B cells, $F(ab')_2$ (1); wt B cells, $F(ab')_2$ (2); Ali5 B cells, thapsigargin (3); and wt B cells, thapsigargin (4).

(E) Indo-1 Ca^{2+} measurement and U73122 Plc inhibition in primary B cells from hybrid B6C3. B cells from heterozygous Plcg2$^{+/Ali5}$ (1) and homozygous Plcg2$^{Ali5/Ali5}$ (2), and wt mice were stimulated by anti-IgM (3). Spleen cells were loaded with Indo-1 as described and activated in Ca^{2+} containing buffer. 0.2 μM U73122 Plc inhibitor was added to heterozygous Plcg2$^{+/Ali5}$ (4), homozygous Plcg2$^{Ali5/Ali5}$ (5), and wt cells (6). Bottom panel shows a magnification of Ca^{2+} signal with U73122 inhibitor. Values are the ratio of signal from Ca^{2+} bound Indo1 (F6) to free Indo-1 (F7).

on interactions with other cells derived from bone marrow, e.g. macrophages, would need to be addressed with mixed bone marrow chimeras as in SHP-1 deficient mice (Cyster and Goodnow, 1995).

As an increased absolute number of granulocytes and macrophages alone would not appear to explain the disease in *Plcg2*^{Ali5} mice, we investigated whether functional differences occur in granulocytes, macrophages, or dendritic cells (DCs). Granulocytes from the peritoneal cavity of C3H *Plcg2*$^{Ali5/+}$ and wt controls exhibit similar phagocytosis of fluorescence-labeled *E. coli* (data not shown). Bone marrow-derived macrophages and DCs were stimulated with various toll-like receptor ligands, e.g. LPS, R-848, poly I:C, and CpG oligo-DNA (Beutler et al., 2003), but no differences in inflammatory cytokine production or upregulation of activation markers were observed (data not shown). In addition, a model of abdominal sepsis (colon ascendens stent peritonitis) (Zantl et al., 1998) and TNCB-mediated contact dermatitis-induced skin inflammation resulted in responses similar to wt mice both in and ex vivo (data not shown). On the other hand, the stimulation of Gr1-positive granulocytes from peripheral blood of C3H Ali5 mice via the FcγR results in sustained Ca^{2+} mobilization similar to that observed in B cells (Figure 5C).

These results confirm a role of Plcγ2 signals in expansion of inflammatory cells but make it unlikely that toll-like receptor-mediated inflammatory pathways are involved in targeting of the inflammatory reaction. Transfer of bone marrow from a homozygous *Plcg2*$^{Ali5/Ali5}$ mouse, which contains few lymphocytes but high numbers of granulocyte-macrophage precursors, leads to induction of paw-specific inflammation.

Lymphocyte-Independent Arthritis and Dermatitis in C3HeB/FeJ *Plcg2*$^{Ali5/+}$ Mice

In order to resolve the specific contribution of lymphocytes and non-B, non-T cells to the induction of the paw-specific arthritis and dermatitis, we mated *Plcg2*$^{Ali5/+}$ heterozygous mice on the C3H genetic background with *Rag1*-deficient mice lacking B and T cells (Mombaerts et al., 1992). *Plcg2*$^{Ali5/+}$*Rag1*$^{-/-}$ mice develop paw inflammation (Figure 6A), even with a higher frequency than their *Plcg2*$^{Ali5/+}$*Rag1*$^{+/+}$ positive littermates (70% versus 30%). As expected, *Plcg2*$^{Ali5/+}$ *Rag1*$^{-/-}$ spleen did not contain follicular structures and lacked B cells completely (Figure 6B, 3 and 4). The primary follicles of *Plcg2*$^{Ali5/+}$*Rag1*$^{+/+}$ contained less B cells than the *Plcg2*$^{+/+}$ *Rag1*$^{+/+}$ wt spleen (Figure 6B, 3).

This shows that dermatitis and arthritis are not mediated by, or dependent on, specific B or T cell populations. Autoreactive T cell responses or autoantibodies seem not to be involved in the inflammatory paw phenotype induced by *Plcg2*^{Ali5}. This suggests that non-B non-T cells originating in the bone marrow expressing the mutant *Plcg2* allele are the inducer and effector cells of the inflammatory pathology in vivo.

A Hyperreactive B Cell Phenotype Occurs in Both C3HeB/FeJ and Hybrid C57BL/6J × C3HeB/FeJ Mice, but Autoantibody Production and Glomerulonephritis are Restricted to Hybrid Mice

Previous studies of Plcg2 in *Plcg2*-deficient mice highlighted its importance in acute responses and develop-

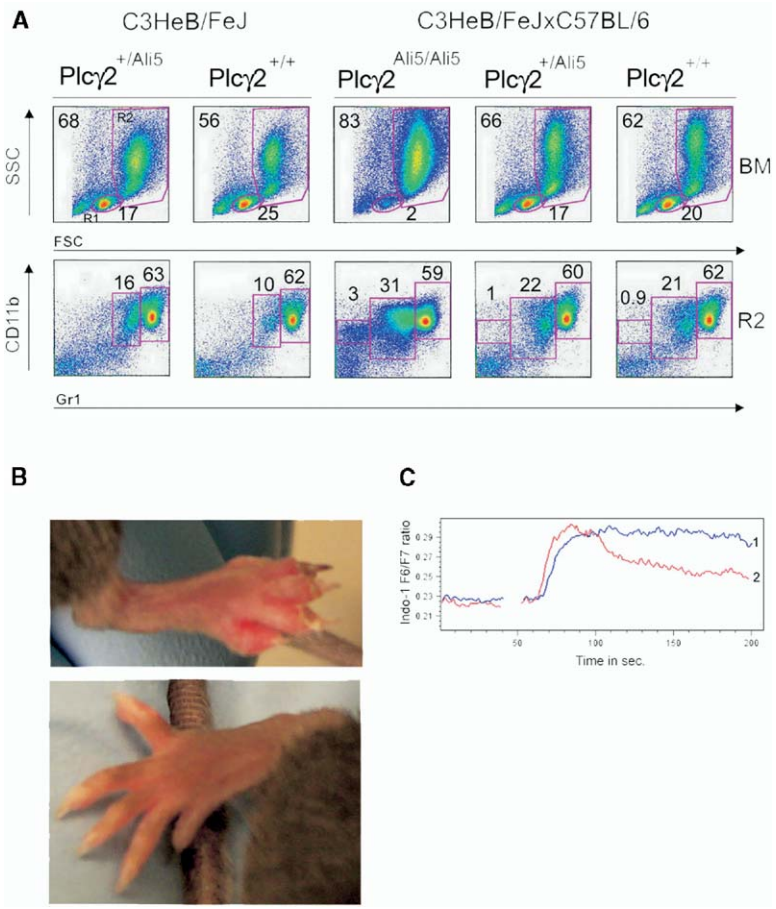

Figure 5. Innate Immune Cell Production in Bone Marrow of Ali5 Mice and Transfer of the Inflammatory Pathology to Wt Mice by Ali5 Bone Marrow Transfer

(A) Flow cytometric analysis of bone marrow cells. Numbers indicate the percentage of gated populations of lymphocytes. Top panels show forward scatter (FSC) versus side scatter (SSC) of bone marrow cells (BM). (R1) contains lymphocytes and (R2) the larger and more granular cells. The bottom panel shows cells gated through R2. Macrophage-CD11b^{+}(Gr-1$^{low/negative}$) and granulocyte-CD11b^{+}(Gr1^{high}) precursors.

(B) Paw inflammation in a wt BL/6 mouse transferred with bone marrow cells from an *Plcg2*$^{Ali5/Ali5}$ mouse (top photo) 4 weeks after transfer and healthy paw in a mouse transferred with wt bone marrow (bottom photo).

(C) Indo-1 Ca^{2+} measurement of granulocytes from peripheral blood of C3H mice. Gr1-positive cells from heterozygous *Plcg2*$^{+/Ali5}$ (1) and wt mice (2) were stimulated via the FcγR. Blood cells were loaded with Indo-1 as described and activated in Ca^{2+} containing buffer. Values are the ratio of signal from Ca^{2+} bound Indo1(F6) to free Indo-1 (F7).

ment of B cells (Hashimoto et al., 2000; Wang et al., 2000). Analysis of Ali5 mice revealed a reduction in the B2 cell population resulting in a higher T cell to mature B cell (CD23^{+}) ratio in blood (Figure 2A). A reduction of mature B cells and transitional T2 B cells (Loder et al., 1999) below 30% of the wt numbers was found in inbred C3H *Plcg2*$^{Ali5/+}$ and B6C3 hybrid *Plcg2*$^{Ali5/Ali5}$ splenocytes (Figure 7A).

Further FACS analysis between wt and mutant mice revealed that the decrease in B cells is at the expense of the CD21^{int} CD23^{hi} follicular B cells (FB) in spleen and leads to a relative increase in CD21^{hi}CD23^{lo} marginal zone (MZ) B cells (Oliver et al., 1999) (Figure 7A). In this context, it is notable that a fundamental strain difference between wt C3H and BL/6 in spleen is that C3H have a higher proportion of MZ B cells (30% versus 10%) but a lower percentage of total B cells (~35% versus 55%) than B6 mice. In C3H mice, this leads to the fact that about 60% of the B cells from Plcgγ2$^{+/Ali5}$ mice display the MZ phenotype (see also Discussion).

In contrast to decreased B2 cells, but in line with the proportional increase of MZ B cells in spleen, the distinct B1 population in the peritoneum is enlarged rather then reduced by the effects of the mutated *Plcg2*^{Ali5} (Figure 7A). This does not lead to an absolute increase of B1 or MZ B cell numbers, because although the number of peritoneal cells and splenocytes is comparable between Ali5 and wt controls, the Ali5 mice contain increased numbers of larger and more granuled cells outside the lymphocyte gate (data not shown). Furthermore, the B1-MZ B cell populations are decreasing in homozygous mice (Figure 7A), probably due to stronger negative selection, which affects the relative-resistant B1-MZ subsets.

Serum immunoglobulin levels were not significantly changed, with the exception of increased IgM in male C3H Ali5 mice (Figure 7C). The response in vitro to the mitogens LPS, anti-CD40, and IL-4 plus anti-IgM, known to be dependent of PLCγ function (Wang et al., 2000), was higher for splenic B cells from inbred C3H *Plcg2*$^{Ali5/+}$ mice than in wt counterparts (Figure 7B). These data show that the remaining mature B cells with the mutated *Plcg2*^{Ali5} are hyperresponsive to B cell mitogens and suggest that they are also hyperreactive to further BCR activation. To examine this hypothesis, we immunized the inbred mice and also examined autoantibody production. Immunization of inbred C3H *Plcg2*$^{Ali5/+}$ mice and control littermates with a T-dependent antigen showed comparable levels of specific antibodies for IgM and IgG_1, despite the reduced B cell numbers of Ali5 mice (Figure 7D). However, the IgG2a- and IgG3-specific antibodies were reduced in Ali5.

T-independent antibody responses were slightly increased in C3H Ali5 mice (Figure 7D). This is consistent with a relative increase of MZ B cells in the spleen. Anti-DNA antibodies were not detected in *Plcg2*$^{Ali5/+}$ mice

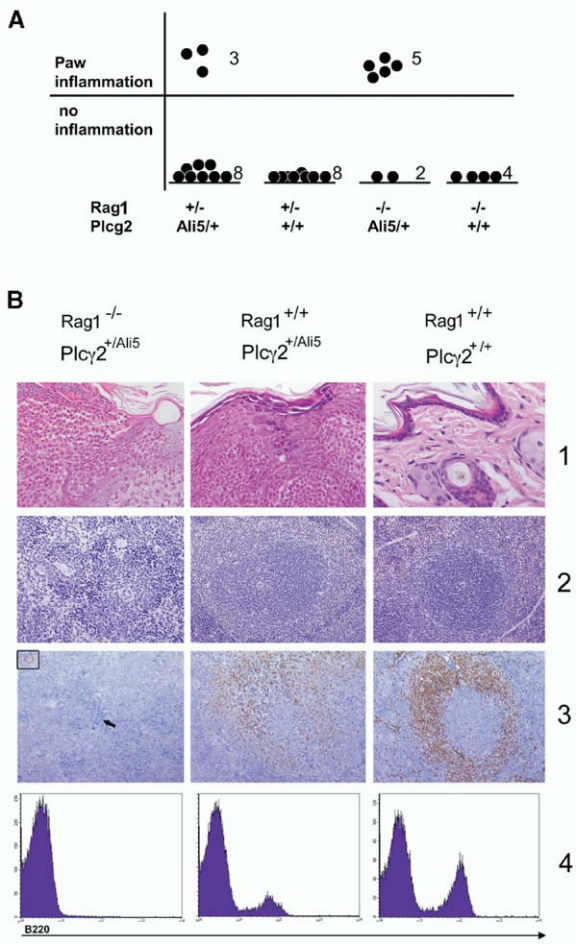

Figure 6. Lymphocyte-Independent Inflammatory Pathology in Rag1$^{-/-}$ Plcg2$^{+/Ali5}$ Mice

(A) Inflammation score of Rag1-deficient C3H Plcg2$^{+/Ali5}$ mice at the age of 6–8 weeks. Macroscopically visible swollen, inflamed footpads develop in Plcg2$^{+/Ali5}$ on both the heterozygous and Rag1-deficient background.

(B) Phenotypical analysis of Rag1-deficient C3H Plcg2$^{+/Ali5}$ mice. Panels in row 1 show histological analysis of an HE staining of an inflamed footpad (320×) of a Rag1$^{-/-}$ Plcg2$^{+/Ali5}$ mouse (left column) and corresponding spleen sections (row 2; HE). Row 3 is immunhistochemical staining with anti-B220 B cell marker on spleen sections (200×). The arrow indicates the position of the arteriole, where exclusively granulocytes are observed. Rare B220-positive cells are identified in the spleen (insert, 640×). Middle column shows a Rag1$^{+/+}$ Plcg2$^{+/Ali5}$ mouse. There is severe inflammation of the skin (320×). Note that Rag1$^{+/+}$ Plcg2$^{+/Ali5}$ mouse has lymphocyte follicles in the spleen (100×) with a reduced number of B220/CD45R-positive B cells, when compared to the wt mouse (right). FACS analysis of peripheral blood with anti-B220 (row 4) confirms absence of B cells in Rag1$^{-/-}$ Plcg2$^{+/Ali5}$ and reduced B cell numbers in Rag1$^{+/+}$ Plcg2$^{+/Ali5}$ compared to the wt mouse.

on the inbred C3H background. However, 28% of *Plcg2*$^{Ali5/+}$ and 66% of *Plcg2*$^{Ali5/Ali5}$ hybrid mice exhibit high anti-DNA antibody titers of the IgG isotype (Figure 7E). Thus, there appears to be in vivo evidence for hyperresponsiveness of B cells. Further, *Plcg2*$^{Ali5/+}$ and *Plcg2*$^{Ali5/Ali5}$ hybrid Ali5 mice develop glomerulonephritis. The penetrance was 30% and 100% in *Plcg2*$^{Ali5/+}$ and *Plcg2*$^{Ali5/Ali5}$ mice, respectively. This correlates with the presence of autoantibodies and supports the notion of autoimmunity resulting in glomerulonephritis due to immune complex deposition in the kidney.

Discussion

In this study, we describe a gain-of–function mutation in *Plcg2* that is linked to signaling and functional deregulation of the immune system in vivo. Furthermore, the analysis of mice with this mutation validates the ENU approach to provide insights into mechanisms leading to autoimmunity and inflammation (Vinuesa and Goodnow, 2004) as well as highlighting the importance of complex genetic interactions in such disorders.

Within the signaling context of B cells, the mutation in *Plcg2*^{Ali5} causes increased and sustained calcium responses with an influx of extracellular calcium as the dominating component. Previous studies implicated PLC in regulation of calcium influx by several mechanisms (Putney, 2002; Putney et al., 2001). The best-documented mechanism involves PI-3K- and Btk-mediated activation of Plcγ2 that results in IP_3 production leading to calcium influx into the cytoplasm from internal endoplasmatic reticulum stores and later through store-operated channels (SOCs) of the plasma membrane. Recently, in vitro experiments using the DT40 cell line showed that PLCγ1 and PLCγ2 can control external Ca^{2+} entry mediated by plasma membrane calcium channels. Surprisingly, a lipase-deficient mutant, PLCγ, was active, presumably functioning independently from the secondary messengers it usually generates (Patterson et al., 2002). This lack of an absolute requirement of PLCγ's catalytic function implies an additional direct influence of PLCγ on the classical SOCs or store-depletion-independent calcium channels (Putney, 2002).

Although the precise changes that underlie enhanced calcium signals by Plcγ2^{Ali5} need to be elucidated further, our data suggest the possibility that the *Plcg2*^{Ali5} mutation could involve several mechanisms. First, increased stability and penetrability at the plasma membrane could result in enhanced and sustained signaling. The mutation is present at the surface region of the catalytic domain that normally restricts membrane interactions. Mutations in this region in PLCδ1 have been reported to enhance such interactions (Ellis et al., 1998). The amino acid change D993G removes a negative charge from a critical region of the molecule that has to come into close proximity with the inner plasma membrane, which is negatively charged. One possibility might therefore be a reduced repulsion of the mutated Plcγ2. As a consequence, this would result in the increase in membrane stability of Plcγ2^{Ali5} that we observed. This could mimic the stabilization normally provided by PIP_3. It is well documented that PIP_3 interacts with the PH domain of Plcg2 to target it to the membrane and therefore allows sustained Ca^{2+} flux (Scharenberg and Kinet, 1998). One way to regulate Plcγ2 function seems to be degradation of PIP_3 by the phosphatase activity of SHIP, resulting in release of Plcγ2 from the membrane and termination of the Ca^{2+} signal. Because SHIP is recruited by the inhibitory FcγRIIb (Ravetch and Bolland, 2001; Scharenberg and Kinet, 1998),

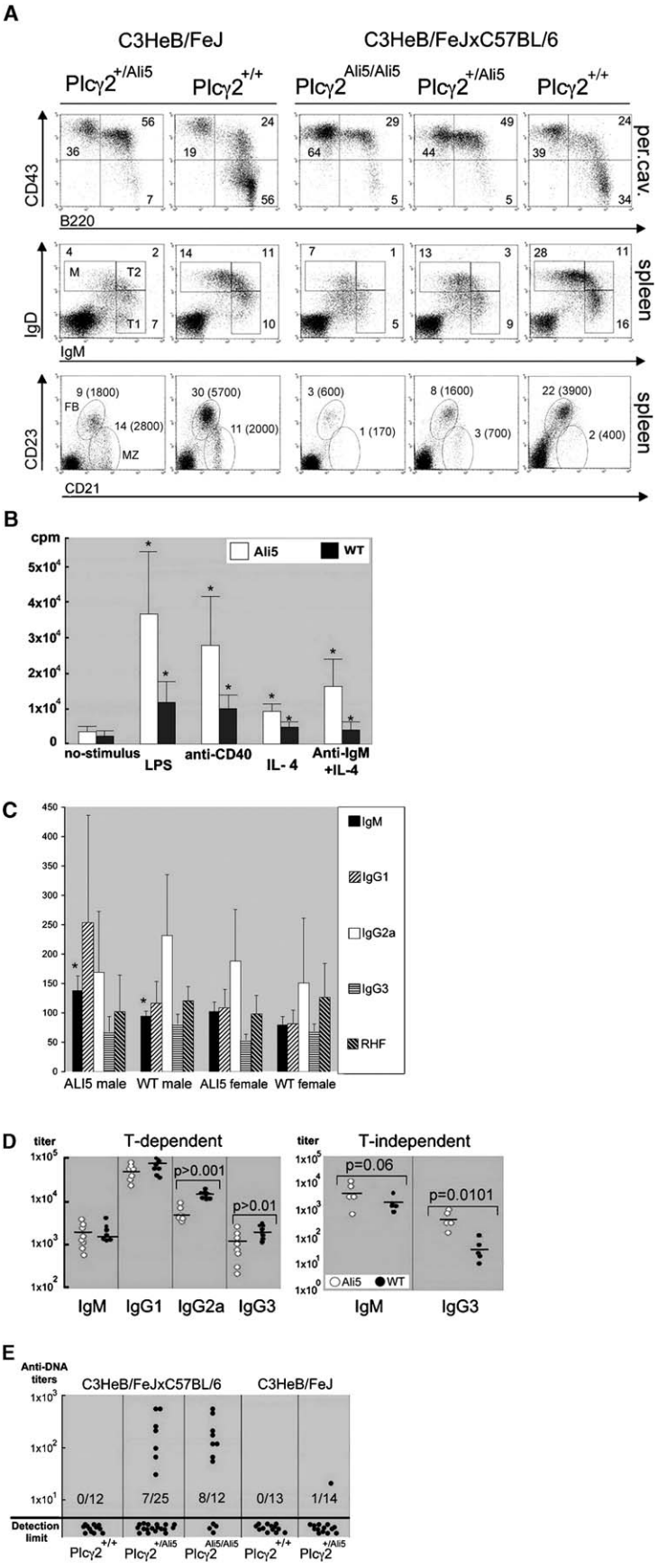

Figure 7. B Cell Phenotype and Function in Plcg2^{Ali5} Mice

(A) In the top panels, the staining with anti-CD43 versus anti-B220 of peritoneal lymphocytes (10,000 cells in the lymphocyte gate) defines B1 cells (CD43^{+}B220^{+}) and B2 cells (CD43^{-}B220^{+}). Middle panels show analysis of B cell populations in spleen (~19,000 cells in the lymphocyte gate) by anti-IgM/anti-IgD staining. The gates correspond to mature (M), transitional 1 (T1) and transitional 2 (T2) B cells. Bottom panels show CD21^{hi}CD23^{lo} marginal zone (MZ) B cells and CD21^{int} CD23^{hi} follicular B cells (FB). Numbers are a percentage of gated cells; in brackets are cell numbers.

(B) Proliferation assay with B220^{+}-purified B cells of inbred C3H *Plcg2*$^{+/Ali5}$ and wt littermates. ^{3}H-thymidine incorporation of cells stimulated with the depicted stimuli. Differences marked with an asterisk are statistically significant ($p < 0.01$). Error bars represent the SD for n = 4 mice per group.

(C) Serum immunoglobulin levels for male and female C3H inbred *Plcg2*$^{+/Ali5}$ and wt littermates. IgM, IgG isotypes, and rheumafactor (anti-IgG Ab, RHF) are depicted. Error bars represent the SD for n = 6 mice per group.

(D) Immunization of C3H-inbred *Plcg2*$^{+/Ali5}$ and wt littermates with the T-dependent antigen ovalbumin and T-independent antigen pneumococcal polysaccharide.

(E) Serum levels of anti-DNA IgG autoantibodies.

the marked increase in Ca^{2+} flux in cells from $Plcg2^{Ali5}$ mice when a FcγRIIb-engaging complete Ab is used for BCR stimulation argues for an independency of $Plcγ2^{Ali5}$ from PIP_3-dependent membrane localization. As a consequence, the enzyme could have prolonged access to its substrate. The similarity of the Km values of recombinant wt and Ali5 mutant Plcg2 protein further supports a more general role in the membrane interactions rather than substrate recognition.

Second, the other possibility is that not all Ca^{2+} responses could be attributed to the differences in enzyme activity in cells and IP_3 production. The mutation might positively affect the functional juxtaposition of a postulated signaling complex containing the adaptors (Grb2/NTAL/SLP-65), Btk, Plcγ2, and an unknown calcium channel (Putney, 2002; Stork et al., 2004). This could lead to the observed specific difference in Ca^{2+} channel-mediated external Ca^{2+} influx without the involvement of Plcγ2's lipase activity. The importance of this protein-protein interaction in controlling Ca^{2+} entry has recently been demonstrated by PLCγ1 directly regulating the TRPC3 Ca^{2+} channel via a novel partial PH domain interaction (van Rossum et al., 2005).

Inhibition of the mutant $Plcγ2^{Ali5}$ using the pharmacological agent U73122 is difficult to interpret but nevertheless important. First, we show that the PLC inhibitor U73122 is able to almost completely block PLC activity in both heterozygous and homozygous mutant B cells, thus demonstrating that the mutant protein is sensitive to a known PLC inhibitor and that PLC activity is essential for the enhanced response observed in mutant cells. Second, it is known that the PLC-specific inhibitor U73122 may also have additional inhibitory effects on certain Ca^{2+} channels (Taylor and Broad, 1998), which could be direct targets for Plcγ2.

It has been shown that mutations in the BCR signaling pathway resulting in stronger BCR signals and elevated Ca^{2+} responses have an impact on B cell development (Marshall et al., 2000). By analogy, the effect of the $Plcg2^{Ali5}$ mutation in B cells can be explained in terms of altered negative and positive selection acting on emerging B cells. Mutant mice with a reduced number of mature B cells that are hyperresponsive to various B cell signals have been described (Marshall et al., 2000). In such circumstances, an increased signal strength through the BCR during negative selection results in a reduced threshold for deletion of mature B2 cells after the T1 stage (Loder et al., 1999), resulting in less mature B cells, similar to the situation in Ali5 mice. However, the B1 cell lineage, and to some extent MZ B cells, seem to be less sensitive to negative selection processes and are not deleted but expand during positive selection (Berland and Wortis, 2002), providing an explanation for the relative increase of these cells in Ali5 mice.

The surprising finding of an increased proliferative response to a toll-like receptor ligand, LPS, and a CD40 signal in $Plcg2^{Ali5}$ mice has two possible nonexclusive explanations. First, ligand-indepedent tonic signaling from the BCR could lead to a synergistic activation signal in vivo and in vitro (Monroe, 2004). Second, it has been reported that MZ B cells respond with increased proliferative response to LPS and anti-CD40 compared to FB cells (B2 B cells) (Oliver et al., 1999). The proportional increase of MZ B cells in C3H Ali5 mice may be reflected in an increased proliferation of $B220^+$ splenic B cells. It is particularly interesting that our results suggest that signaling via Plcγ2 does have an indirect effect on both LPS and CD40 signaling, probably by affecting B cell lineage selection, although neither of these ligands is known to directly activate Plcγ2. Analogous conclusions can be drawn from impaired proliferative responses of splenic B cells of Plcγ2-deficient mice (Wang et al., 2000).

There are several ways that these B cell changes could lead to a breakdown in tolerance. First, the remaining mature B cells respond with an elevated response to BCR signals. If a mature B cell escapes negative selection and is still able to recognize self-antigen, the response would be increased, leading to B cell expansion and production of autoantibodies. This is reflected in Ali5 mice in a relatively strong specific antibody response and induction of autoantibody production that ultimately leads to immune complex glomerulonephritis in the B6C3 background. Second, the remaining numbers of MZ B cells and B1 cells might be responsible. B1 cells have been associated with self-reactivity (Berland and Wortis, 2002). B1 cells produce primarily IgM, and levels were higher in Ali5 male mice on the C3H background compared to wt controls. Regardless of the cell type responsible, it is still surprising how a single mutation in *Plcg2* can break the mechanisms regulating self-tolerance (Halverson et al., 2004). Although there is evidence that clonal deletion operates in bone marrow and spleen of Ali5 mice, other peripheral mechanisms of B cell tolerance like anergy or receptor editing await analysis.

The cell phenotype in Ali5 mice is consistent with a gain-of-function mutation in Plcg2 and is supported by the previously reported immunological phenotype in *Plcg2*-deficient mice, which is diametrically opposed to Ali5. Ca^{2+} mobilization is completely lacking in B cells after BCR activation, the proliferative response to in vitro B cell stimulation is reduced, B1 cells are absent from the peritoneum, and they fail to respond to T-independent antigens (Hashimoto et al., 2000; Kurosaki et al., 2000; Marshall et al., 2000; Wang et al., 2000). The Ali5 phenotype, particularly the duality of inflammation and B cell autoimmunity, displays striking similarities with the mouse mutants of the tyrosine kinase *Lyn* and the phosphatase Shp-1 (*Me/Me^v*) (Hibbs et al., 2002; Shultz et al., 1997). Both molecules regulate Plcγ2, and mutant B cells respond with enhanced Ca^{2+} signaling. Although the restricted expression of *Lyn* to B cells might limit the disease phenotype to immune complex glomerulonephritis, lethal inflammation and autoantibody production are also present in *Me/Me^v* mice, probably because of the loss of the even wider inhibitory function of Shp-1 in macrophages and granulocytes. An additional similarity is the complete lymphocyte independency of the inflammation in both $Plcg2^{Ali5}$ and $Shp\text{-}1^{Me/Mev}$ mice (Yu et al., 1996). The Ali5 phenotype suggests that Plcγ2 is an important downstream molecule in *Lyn* gain-of-function and $Shp\text{-}1^{Me/Mev}$-driven disease.

Although the role of Plcγ2 is comparably well understood in B cells, the understanding of its function and integration in signaling pathways of other cells is lim-

ited. Plcg2 is primarily expressed in haematopoietic cells (Wang et al., 2000). The dermatitis and arthritis in Ali5 mice are independent of B and T cells but dependent on a transferable bone marrow-derived haematopoietic cell population. The transfer of bone marrow from a *Plcg2*$^{Ali5/Ali5}$ homozygous mouse, which consists mainly of macrophage/granulocyte precursors, leads to paw inflammation evident within 4 weeks of transfer.

Plcg2 is expressed in mast cells and monocytes/macrophages and is activated by crosslinking of FcεRI and activating Fcγ receptors, resulting in an elevation in intracellular Ca^{2+} levels. *Plcg2*-deficient mice have normal numbers of these cells, but FcεRI- and FcγR-mediated processes, such as FcγR-mediated phagocytosis in macrophages and FcγR-mediated passive skin inflammation induced by mast cells, are impaired (Wen et al., 2002). Given this, it seems possible that lowering of the threshold for an activation signal in these cells could result in the acquisition of autoreactive behavior. Certainly, the triggering of tissue-specific inflammation seems to involve an increased production of granulocytes/macrophages cells in *Plcg2*^{Ali5} mice, which could depend on increased M-CSF receptor signaling (Bourette et al., 1997). The proof that granulocytes also respond with increased Ca^{2+} flux to FcγR stimulation implies that a pathway, involving Plcγ2, exists that drives and/or directs these cells during inflammation. However, the exact nature of the stimulus that targets the inflammation to restricted areas of the body remains to be determined together with the exact role of implied signaling pathways (FcγR, M-CSF R, and FcεRI) that recruit Plcγ2 in these cells in an autoimmune-inflammatory process. Failure to trigger an enhanced response of inflammatory cells from Ali5 mice in vitro by various microbial toll-like receptor ligands and in vivo by two inflammatory stimuli underlines the enigmatic nature of the initial trigger that leads to specific autoaggressive reactions.

One of the commonly accepted theories of autoimmunity focuses on the function of autoreactive helper T cells, which might drive the disease by induction of organ-specific inflammatory processes (Khoury and Sayegh, 2004; Mathis and Benoist, 2004). The K/BxN-TCR-transgenic mouse model and a mouse mutant with a point mutation in the signaling molecule ZAP-70 both develop symptoms similar to rheumatoid arthritis in humans (Korganow et al., 1999; Sakaguchi et al., 2003), pointing to autoreactive T cells as the initial trigger for the autoimmune process. The Lyn, Shp-1, and particularly Ali5 mutants contrast with this model. The mechanism leading to both inflammatory disease and B cell-mediated autoimmunity in the Ali5 mouse must be different, because *Plcg2* appears not to be involved in T cell function (Emori et al., 1989; Wilde and Watson, 2001), and the paw inflammation occurs in the absence of B or T cells. It might involve a direct activation of B cells (Martin and Chan, 2004) and haematopoietic non-B, non-T cells.

Functional experiments with samples from patients will be necessary to examine if similar signaling pathways might be engaged in human disease. The Ali5 phenotype seems not to be directly comparable to a single human illness such as WG, rheumatoid arthritis, or SLE (Martin and Chan, 2004), and genetic linkage analysis has yet to reveal an association of *PLCG2* or its signaling pathway with these diseases.

Nevertheless, in particular, human SLE might share a common mechanism of B cell hyperactivity (Lipsky, 2001) and diagnostic criteria as dermatitis, increased Ca^{2+} mobilization in B cells (Liossis et al., 1996) and immune complex glomerulonephritis with the murine *Plcg2*^{Ali5} phenotype.

Another similarity between the *Plcg2*^{Ali5} phenotype and the human situation is the complex genetics, because unexpectedly, a change in the genetic background from C3H to hybrid C3B6 dramatically altered the pathology in heterozygous Ali5 mice. The change from inflammation to B cell autoimmunity in the mixed genetic background is accompanied by regaining of in vitro-fertilizing capacity of sperm and male fertility (P.Y., N.D., U.H., S.K., L.Q.-M., unpublished data). Thus, modifier genes must exist in the different genetic backgrounds that are able to differentially control *Plcg2*^{Ali5}-driven disease. Additionally, the phenotype of the homozygous mice on the different genetic backgrounds implies a gene-dosage effect of the *Plcg2*^{Ali5} mutant allele that can overcome the effect of modifiers.

In conclusion, we provide evidence that an enhanced signal in vivo by a member of the phospholipase C family of signaling molecules leads to severe pathology that is similar to a variety of human inflammatory-autoimmune diseases. Thus, an autoimmune-inflammatory pathology can be induced by a single mutation in a key signaling molecule that targets external Ca^{2+} influx. Additionally, other, as yet unknown, genes can extensively modulate the severity of the induced disease. Our findings indicate that mutations in loci of the genes encoding signaling molecules in B cells and haematopoietic non-B, non-T cells also contribute to autoimmunity and inflammation. This mouse model will enable further analysis of the role of Plcg2 and its genetic modifiers in complex genetic inflammatory-autoimmune diseases.

Experimental Procedures

ENU Mutagenesis and Mice

ENU mutagenesis of C3HeB/FeJ male mice was performed as previously described (Hrabe de Angelis et al., 2000). C3H Ali5-affected female mice were mated to C3H wt males, and the heterozygous offspring were used for analysis. In addition, crossing to C57BL/6J wt male mice was performed for positional cloning and further analysis. *Rag1*-deficient mice on the C3H background were obtained from I. Förster, TUM, and used for mating with C3H inbred *Plcg2*$^{Ali5/+}$ mice. The phenotype was confirmed by FACS. In the bone marrow transfer, 1.5×10^6 cells from a hybrid B6C3 *Plcg2*$^{Ali5/Ali5}$ mouse were injected i.v. into wt recipients, which were lethally irradiated by a split dose of 2 × 500 Gray and treated with the antibiotic Polymyxin B (Sigma).

Identification of the Mutation by Positional Cloning

To map the mutation, an outcross and backcross strategy was followed. Female C3HeB/FeJ mice demonstrating the Ali5 phenotype were outcrossed to C57BL6/J, and the resulting N_1 hybrids were backcrossed again to C57BL6/J. For chromosomal localization, equal amounts of DNA extracted from tail biopsies of 12 unaffected N_2 mice were pooled. The allele frequency of this pooled sample was determined for 90 equally spaced genome wide-distributed single-nucleotide polymorphic (SNP) markers by using a Luc96 pyrosequencer (Pyrosequencing AB). After this initial mapping, unaffected and affected mice were typed individually to confirm the map location and narrow down the region by the analysis of single

recombination events. As the ratio of T cell versus mature B cells is a fully penetrant phenotype in N_1 and N_2 animals, in contrast to the paw phenotype, recombination events in affected and unaffected animals could be used for mapping. The fine mapping was based on 422 meiotic events and finally reduced the locus to 1.3 Mb between the microsatellite markers D8Ing65 (PCR primer D8Ing65-F, 5′-GCCTCAGCCTACTCTGAC-3′ and PCR primer D8Ing65-R, 5′-CTGACGTCAATGTTACCATG-3′) and D8Ing60 (PCR primer D8Ing60-F, 5′-GCTAAGATACAGGCATGGTTCG-3′ and PCR primer D8Ing60-R, 5′-TTCCAGGAGGTGGAAAGAAGAG-3′). Several candidate genes, including *Plcg2*, in the region were sequenced at the genomic and cDNA levels. The genomic structure of *Plcg2* (33 exons) was deduced from known spliced mouse ESTs, public rat (NM_017168), and human (XM_051778; NM_002661) *PLCG2*.

Plcg2^{Ali5} Gene Expression

RNA expression of CD45R/B220-positive B cells (purified by MACS Miltenyi, Germany) was examined in a pool of ten inbred C3HeB/FeJ *Plcg2$^{Ali5/+}$* and five *Plcg2$^{+/+}$* littermate mice. Expression of *Plcg2* and four dysregulated genes were tested by light cycler quantitative PCR (Boehringer). The primers for *Plcg2* were: A: 5′-CCTTTACGACACGCACCAG-3′, B: 5′-CACGGTGTTCACGAGCGC-3′; S100A9, A: 5′-GTTGGGCAGCAGTCACATGG-3′, B: 5′-CAG ACAAATGGTGGAAGCACAG;S100A6-3′; A: 5′-CCCTGAGCAAG AAGGAGCTG-3′, B: 5′-GGAAGTCATCTCAACGGTCC-3′; MEK1 (Map2k), A: 5′-GAAGCAGCTCATGGTACATGC-3′, B: 5′-GCAACA TGGCATGCCACTGGG-3′; *Iga*, A: 5′-GTCAGTCATGGCTTTTCCAGC-3′, B: 5′-GCAGTGGTGCCAGGGACGCTG-3′; and Housekeeping gene *b2microglobulin*, A: 5′-CCTCACATTGAAATCCAAATGCTGA-3′, B: 5′-TCTTGGGCTCGGCCATACT-3′; the B cell-specific gene *Cd19* primers A: 5′-CAGCATGGGAAGGAGAGG-3′, B: 5′-GCT TTGCTTGAACATGCATATG-3′, and C: 5′-GCTTCAGAGAATTTGAG TGGC-3′ were used as standards. Western blots for Plcγ2 detection were done by standard procedure using a goat anti-Plcγ2 serum (Santa Cruz).

Histology, Immunohistochemistry, X-Ray Analysis, and Electron Microscopy

Organs were fixed in 4% (w/v) formaldehyde. Paraffin-embedded tissue sections (3 μm) were stained with haematoxylin and eosin and with giemsa or PAS where indicated. Bones were decalcified in EDTA for at least 6 weeks. Paraffin-embedded spleen sections were analyzed for expression of B220/CD45R (BD Pharmingen, Heidelberg, Germany) by using an automated immunostainer (Ventana Medical Systems, Strasbourg Cedex, France) per the manufacturer's protocol. Animals were analyzed by X-ray (Faxitron Cabinet X-Ray System) in order to document the presence of bone changes. Kidney tissue was fixed in 3% (w/v) glutaraldehyde and examined by transmission electron microscopy.

Flow Cytometry and Calcium Fluorimetry

Cells were stained with combinations of anti-IgD, anti-IgM, anti-CD45R/B220, anti-CD3, anti-CD43, anti-CD23, anti-CD11b, and anti-Gr-1 (Ly6G). Monoclonal antibodies conjugated to fluorescein isothiocyanate, phycoerythrin (PE), or allophycocyanin (APC) were obtained from Pharmingen. Analysis was done on a FACScalibur (Becton Dickinson) and a Cyan (Dako Cytomation). Calcium monitoring was done in spleen cells at 2×10^6 cells in a volume 400 μl. They were loaded with 2 μM Fluo-3, Fura-Red, or 10 μM Indo-1 (Molecular Probes) in HBSS buffer for 40 min at room temperature and stained with anti-B220-APC. For T cell activation, loaded cells were stained at 4°C with anti-CD90-PE and rat-anti-TCRβ (H57-597) at a concentration of 10 μg/ml. Calcium fluorescence was determined in B220- or CD90-positive cells by flow cytometry. B cells were stimulated by 15 μg goat anti-IgM (Star86, Serotech) antibody or 19.5 μg goat anti-IgM $F(ab)_2$ fragment (Jackson ImmunoResearch). Inhibition of Ca^{2+} flux was done at 0.2 μM concentration of U73122 (Biomol) for 5 min at 37°C. Peripheral blood cells were stained with Ly6G anti-Gr1 and Fc Block (2.4G2, Becton Dickinson) and crosslinked by anti-rat IgG (Southern Biotech) as described (Wen et al., 2002). T cells were stimulated by adding 15 μg rabbit anti-rat IgG Ab (Pharmingen). Analysis was done with FlowJo software. In vitro Ca^{2+} mobilization was performed with primary splenic B cells stimulated for 24 hr with 10 μg/ml LPS. Cells were infected in vitro by *Plcg2* wt and mutant cDNA cloned into the MSCV2.2-derived Vector MIGR1 (Pear et al., 1998). Ca^{2+} analysis was done 48 hr after infection. For stimulation experiments without free Ca^{2+}, HBSS without Ca^{2+} was used and 3 mM EGTA was added. Thapsigargin (Sigma) was used at a final concentration of 1 μM.

Proliferation Assay

$B220^+$ splenocytes were positively enriched by MACS according to the manufacturer's guidelines (Miltenyi Biotec). and resulted in 70%–80% purity from C3H Ali5 mice (n = 8) and 90% purity from wt littermates (n = 5). For proliferation assays, 2×10^5 cells per well in flat-bottom 96-well plates were incubated with the following stimuli: LPS (20 μg/ml, Sigma), IL-4 (40 ng/ml, Preprotech), anti-IgM $F(ab)_2$ (2 μg/ml, Jackson ImmunoResearch), and anti-CD40 (1 μg/ml, Pharmingen). Incubation was for 72 hr with the last 14 hr pulsed with 1 μCi/well ^{3}H-dT (Pharmacia).

Immunization and ELISAs

Isotype-specific serum immunoglobulin levels were determined by standard ELISA. Rheuma factor (RHF) antibodies were detected by coating of ELISA plates with mouse IgG1/ lambda light chain Ab (Becton Dickinson). Bound anti-IgG RHF was detected by biotinylated anti-kappa light chain Ab (Dianova).

C3H *Plcg2$^{+/Ali5}$* mice and wt littermate controls 6–8 weeks of age were immunized either intraperitoneally or subcutaneously and boosted 3 weeks later with a total of 100 μg chicken ovalbumin adsorbed to Alum (Fluka). Blood was taken 6 days later, and the serum was separated and used for specific ELISAs. Similarly, specific T-independent responses were measured at day 7 after a single intraperitoneal injection of 10 μg pneumococcal polysaccharide type 19 (American Type Tissue Collection). The values given are specific dilutions at half-maximal optical density. Detection of anti-DNA autoantibodies was performed as described earlier (Flaswinkel et al., 2000). The mice were C3H *Plcg2$^{Ali5/+}$* mice (n = 13, average age 102 days), *Plcg2$^{+/+}$* (n = 13, average age 91 days), hybrid N_1 or N_2 hybrid *Plcg2$^{Ali5/Ali5}$* (n = 12, average age 133 days), *Plcg2$^{Ali5/+}$* (n = 25, average age 113 days), and wt $Plcg2^{+/+}$ (n = 12, average age 123 days). The values given are specific dilutions at half maximal optical density compared to a standard serum of *lpr* mice.

In Vitro PLC Assay and Localization of Membrane-Associated Plcγ2

The recombinant proteins were full-length Plcg2-His_6 constructs of wt and mutated enzyme expressed by using baculovirus as described previously (Rodriguez et al., 2001). The preparations were used for measurements of PLC activity by using detergent-mixed micelles containing sodium cholate and ^{3}H-PIP_2 (Ellis et al., 1998).

Plcγ2 membrane localization studies were done as described previously (Rodriguez et al., 2001). Briefly, cells were homogenized in hypotonic lysis buffer, and after removal of nuclei by centrifugation, supernatants were subjected to further centrifugation at 100,000 × g for 30 min. The precipitates were resuspended in lysis buffer containing 1% Triton X-100 and subjected to centrifugation at 12,000 × g for 20 min, and the resulting supernatants representing particulate/membrane fraction analyzed by Western blotting.

Anti-Calveolin-1 Ab and total Plcγ2 detection were used as membrane and loading control respectively.

Plcg2^{Ali5} Homology Structural Model

The homology model for the X and Y domains of Plcγ2 (Figure 3A) was made with the MOE program and based on the crystal structure of Plcδ1 (Essen et al., 1996). The figure was generated with the molecular modeling program package SYBYL (Tripos Associates, USA).

Acknowledgments

We thank H. Drexler, A. Servatius, N. Sandholzer, Y. Knack, K. Tentschert, U. Mollenhauer, P. Schropp, A. Wunderlich, A. Lohner,

M. Weber, A. Wolf, K. Schneider, S. Stonawski, N. Kink, J. Müller, S. Holthaus, E. Samson, and L. Jennen for excellent technical assistance; E. Yu for help with the figures; J. Kraus and B. Kramer from 4SC, Martinsried, Germany for the 3D model; J. Arnason, G. Häcker, S. Bauer, I. Förster, and H. Kikutani (Osaka, Japan) for helpful discussion; and L. Nitschke (Erlangen, Germany) and D. Wang (Wisconsin, USA) for advice on Ca^{2+} measurements. This work was supported by the Deutsche Forschungsgemeinschaft, SFB 456, SFB 391, NGFN, and a BMBF grant to J.G.

Received: August 1, 2004
Revised: January 7, 2005
Accepted: January 12, 2005
Published: April 19, 2005

References

Berland, R., and Wortis, H.H. (2002). Origins and functions of B-1 cells with notes on the role of CD5. Annu. Rev. Immunol. *20*, 253–300.

Beutler, B., Hoebe, K., Du, X., and Ulevitch, R.J. (2003). How we detect microbes and respond to them: the Toll-like receptors and their transducers. J. Leukoc. Biol. *74*, 479–485.

Bolland, S., and Ravetch, J.V. (2000). Spontaneous autoimmune disease in Fc(gamma)RIIB-deficient mice results from strain-specific epistasis. Immunity *13*, 277–285.

Bourette, R.P., Myles, G.M., Choi, J.L., and Rohrschneider, L.R. (1997). Sequential activation of phoshatidylinositol 3-kinase and phospholipase C-gamma2 by the M-CSF receptor is necessary for differentiation signaling. EMBO J. *16*, 5880–5893.

Coggeshall, K.M., Nakamura, K., and Phee, H. (2002). How do inhibitory phosphatases work? Mol. Immunol. *39*, 521–529.

Cyster, J.G., and Goodnow, C.C. (1995). Protein tyrosine phosphatase 1C negatively regulates antigen receptor signaling in B lymphocytes and determines thresholds for negative selection. Immunity *2*, 13–24.

Ellis, M.V., James, S.R., Perisic, O., Downes, C.P., Williams, R.L., and Katan, M. (1998). Catalytic domain of phosphoinositide-specific phospholipase C (PLC). Mutational analysis of residues within the active site and hydrophobic ridge of plcdelta1. J. Biol. Chem. *273*, 11650–11659.

Emori, Y., Homma, Y., Sorimachi, H., Kawasaki, H., Nakanishi, O., Suzuki, K., and Takenawa, T. (1989). A second type of rat phosphoinositide-specific phospholipase C containing a src-related sequence not essential for phosphoinositide-hydrolyzing activity. J. Biol. Chem. *264*, 21885–21890.

Essen, L.O., Perisic, O., Cheung, R., Katan, M., and Williams, R.L. (1996). Crystal structure of a mammalian phosphoinositide-specific phospholipase C delta. Nature *380*, 595–602.

Flaswinkel, H., Alessandrini, F., Rathkolb, B., Decker, T., Kremmer, E., Servatius, A., Jakob, T., Soewarto, D., Marschall, S., Fella, C., et al. (2000). Identification of immunological relevant phenotypes in ENU mutagenized mice. Mamm. Genome *11*, 526–527.

Halverson, R., Torres, R.M., and Pelanda, R. (2004). Receptor editing is the main mechanism of B cell tolerance toward membrane antigens. Nat. Immunol. *5*, 645–650.

Hashimoto, A., Takeda, K., Inaba, M., Sekimata, M., Kaisho, T., Ikehara, S., Homma, Y., Akira, S., and Kurosaki, T. (2000). Cutting edge: essential role of phospholipase C-gamma 2 in B cell development and function. J. Immunol. *165*, 1738–1742.

Hibbs, M.L., Harder, K.W., Armes, J., Kountouri, N., Quilici, C., Casagranda, F., Dunn, A.R., and Tarlinton, D.M. (2002). Sustained activation of Lyn tyrosine kinase in vivo leads to autoimmunity. J. Exp. Med. *196*, 1593–1604.

Hiller, G., and Sundler, R. (2002). Regulation of phospholipase C-gamma 2 via phosphatidylinositol 3-kinase in macrophages. Cell. Signal. *14*, 169–173.

Horai, R., Saijo, S., Tanioka, H., Nakae, S., Sudo, K., Okahara, A., Ikuse, T., Asano, M., and Iwakura, Y. (2000). Development of chronic inflammatory arthropathy resembling rheumatoid arthritis in interleukin 1 receptor antagonist-deficient mice. J. Exp. Med. *191*, 313–320.

Hrabe de Angelis, M.H., Flaswinkel, H., Fuchs, H., Rathkolb, B., Soewarto, D., Marschall, S., Heffner, S., Pargent, W., Wuensch, K., Jung, M., et al. (2000). Genome-wide, large-scale production of mutant mice by ENU mutagenesis. Nat. Genet. *25*, 444–447.

Hurley, J.H., and Grobler, J.A. (1997). Protein kinase C and phospholipase C: bilayer interactions and regulation. Curr. Opin. Struct. Biol. *7*, 557–565.

Khoury, S.J., and Sayegh, M.H. (2004). The roles of the new negative T cell costimulatory pathways in regulating autoimmunity. Immunity *20*, 529–538.

Korganow, A.S., Ji, H., Mangialaio, S., Duchatelle, V., Pelanda, R., Martin, T., Degott, C., Kikutani, H., Rajewsky, K., Pasquali, J.L., et al. (1999). From systemic T cell self-reactivity to organ-specific autoimmune disease via immunoglobulins. Immunity *10*, 451–461.

Kurosaki, T., Maeda, A., Ishiai, M., Hashimoto, A., Inabe, K., and Takata, M. (2000). Regulation of the phospholipase C-gamma2 pathway in B cells. Immunol. Rev. *176*, 19–29.

Liossis, S.N., Kovacs, B., Dennis, G., Kammer, G.M., and Tsokos, G.C. (1996). B cells from patients with systemic lupus erythematosus display abnormal antigen receptor-mediated early signal transduction events. J. Clin. Invest. *98*, 2549–2557.

Lipsky, P.E. (2001). Systemic lupus erythematosus: an autoimmune disease of B cell hyperactivity. Nat. Immunol. *2*, 764–766.

Loder, F., Mutschler, B., Ray, R.J., Paige, C.J., Sideras, P., Torres, R., Lamers, M.C., and Carsetti, R. (1999). B cell development in the spleen takes place in discrete steps and is determined by the quality of B cell receptor-derived signals. J. Exp. Med. *190*, 75–89.

Marshall, A.J., Niiro, H., Yun, T.J., and Clark, E.A. (2000). Regulation of B-cell activation and differentiation by the phosphatidylinositol 3-kinase and phospholipase Cgamma pathway. Immunol. Rev. *176*, 30–46.

Martin, F., and Chan, A.C. (2004). Pathogenic roles of B cells in human autoimmunity; insights from the clinic. Immunity *20*, 517–527.

Mathis, D., and Benoist, C. (2004). Back to central tolerance. Immunity *20*, 509–516.

Mombaerts, P., Iacomini, J., Johnson, R.S., Herrup, K., Tonegawa, S., and Papaioannou, V.E. (1992). RAG-1-deficient mice have no mature B and T lymphocytes. Cell *68*, 869–877.

Monroe, J.G. (2004). Ligand-independent tonic signaling in B-cell receptor function. Curr. Opin. Immunol. *16*, 288–295.

Nathan, C. (2002). Points of control in inflammation. Nature *420*, 846–852.

Nelms, K.A., and Goodnow, C.C. (2001). Genome-wide ENU mutagenesis to reveal immune regulators. Immunity *15*, 409–418.

Oliver, A.M., Martin, F., and Kearney, J.F. (1999). IgMhighCD21high lymphocytes enriched in the splenic marginal zone generate effector cells more rapidly than the bulk of follicular B cells. J. Immunol. *162*, 7198–7207.

Patterson, R.L., van Rossum, D.B., Ford, D.L., Hurt, K.J., Bae, S.S., Suh, P.G., Kurosaki, T., Snyder, S.H., and Gill, D.L. (2002). Phospholipase C-gamma is required for agonist-induced Ca2+ entry. Cell *111*, 529–541.

Pear, W.S., Miller, J.P., Xu, L., Pui, J.C., Soffer, B., Quackenbush, R.C., Pendergast, A.M., Bronson, R., Aster, J.C., Scott, M.L., and Baltimore, D. (1998). Efficient and rapid induction of a chronic myelogenous leukemia-like myeloproliferative disease in mice receiving P210 bcr/abl-transduced bone marrow. Blood *92*, 3780–3792.

Putney, J.W. (2002). PLC-gamma: an old player has a new role. Nat. Cell Biol. *4*, E280–E281.

Putney, J.W., Jr., Broad, L.M., Braun, F.J., Lievremont, J.P., and Bird, G.S. (2001). Mechanisms of capacitative calcium entry. J. Cell Sci. *114*, 2223–2229.

Ravetch, J.V., and Bolland, S. (2001). IgG Fc receptors. Annu. Rev. Immunol. *19*, 275–290.

Rhee, S.G. (2001). Regulation of phosphoinositide-specific phospholipase C. Annu. Rev. Biochem. *70*, 281–312.

Roberton, C.A., and Vyse, T.J. (2000). The genetics of systemic lupus erythematosus. Exp. Nephrol. *8*, 194–202.

Rodriguez, R., Matsuda, M., Perisic, O., Bravo, J., Paul, A., Jones, N.P., Light, Y., Swann, K., Williams, R.L., and Katan, M. (2001). Tyrosine residues in phospholipase Cgamma 2 essential for the enzyme function in B-cell signaling. J. Biol. Chem. *276*, 47982–47992.

Roth, J., Vogl, T., Sorg, C., and Sunderkotter, C. (2003). Phagocyte-specific S100 proteins: a novel group of proinflammatory molecules. Trends Immunol. *24*, 155–158.

Ryckman, C., Vandal, K., Rouleau, P., Talbot, M., and Tessier, P.A. (2003). Proinflammatory activities of S100: proteins S100A8, S100A9, and S100A8/A9 induce neutrophil chemotaxis and adhesion. J. Immunol. *170*, 3233–3242.

Sack, K., and Fye, K.E. (2001). Rheumatic diseases. In Medical Immunology, T.G. Parslow, D.P. Stites, A.I. Terr, and J.B. Imboden, eds. (New York: Lange Medical Books/McGraw-Hill Medical Publishing Division), pp. 401–420.

Sakaguchi, N., Takahashi, T., Hata, H., Nomura, T., Tagami, T., Yamazaki, S., Sakihama, T., Matsutani, T., Negishi, I., Nakatsuru, S., and Sakaguchi, S. (2003). Altered thymic T-cell selection due to a mutation of the ZAP-70 gene causes autoimmune arthritis in mice. Nature *426*, 454–460.

Scharenberg, A.M., and Kinet, J.P. (1998). PtdIns-3,4,5-P3: a regulatory nexus between tyrosine kinases and sustained calcium signals. Cell *94*, 5–8.

Shultz, L.D., Rajan, T.V., and Greiner, D.L. (1997). Severe defects in immunity and hematopoiesis caused by SHP-1 protein-tyrosine-phosphatase deficiency. Trends Biotechnol. *15*, 302–307.

Stork, B., Engelke, M., Frey, J., Horejsi, V., Hamm-Baarke, A., Schraven, B., Kurosaki, T., and Wienands, J. (2004). Grb2 and the non-T cell activation linker NTAL constitute a Ca(2+)-regulating signal circuit in B lymphocytes. Immunity *21*, 681–691.

Taylor, C.W., and Broad, L.M. (1998). Pharmacological analysis of intracellular Ca2+ signalling: problems and pitfalls. Trends Pharmacol. Sci. *19*, 370–375.

Ueda, H., Howson, J.M., Esposito, L., Heward, J., Snook, H., Chamberlain, G., Rainbow, D.B., Hunter, K.M., Smith, A.N., Di Genova, G., et al. (2003). Association of the T-cell regulatory gene CTLA4 with susceptibility to autoimmune disease. Nature *423*, 506–511.

van Rossum, D.B., Patterson, R.L., Sharma, S., Barrow, R.K., Kornberg, M., Gill, D.L., and Snyder, S.H. (2005). Phospholipase Cgamma1 controls surface expression of TRPC3 through an intermolecular PH domain. Nature *434*, 99–104.

Vinuesa, C.G., and Goodnow, C.C. (2004). Illuminating autoimmune regulators through controlled variation of the mouse genome sequence. Immunity *20*, 669–679.

Wang, D., Feng, J., Wen, R., Marine, J.C., Sangster, M.Y., Parganas, E., Hoffmeyer, A., Jackson, C.W., Cleveland, J.L., Murray, P.J., and Ihle, J.N. (2000). Phospholipase Cgamma2 is essential in the functions of B cell and several Fc receptors. Immunity *13*, 25–35.

Wen, R., Jou, S.T., Chen, Y., Hoffmeyer, A., and Wang, D. (2002). Phospholipase C gamma 2 is essential for specific functions of Fc epsilon R and Fc gamma R. J. Immunol. *169*, 6743–6752.

Wilde, J.I., and Watson, S.P. (2001). Regulation of phospholipase C gamma isoforms in haematopoietic cells: why one, not the other? Cell. Signal. *13*, 691–701.

Wollheim, F.A., Ciusani, E., Acevedo, E., Angulo, J., Castro, F., and Wollheim, M.S. (2003). Genetics and susceptibility to RA--more than HLA. Scand. J. Rheumatol. *32*, 196.

Ye, K., Aghdasi, B., Luo, H.R., Moriarity, J.L., Wu, F.Y., Hong, J.J., Hurt, K.J., Bae, S.S., Suh, P.G., and Snyder, S.H. (2002). Phospholipase C gamma 1 is a physiological guanine nucleotide exchange factor for the nuclear GTPase PIKE. Nature *415*, 541–544.

Yu, C.C., Tsui, H.W., Ngan, B.Y., Shulman, M.J., Wu, G.E., and Tsui, F.W. (1996). B and T cells are not required for the viable motheaten phenotype. J. Exp. Med. *183*, 371–380.

Zantl, N., Uebe, A., Neumann, B., Wagner, H., Siewert, J.R., Holzmann, B., Heidecke, C.D., and Pfeffer, K. (1998). Essential role of gamma interferon in survival of colon ascendens stent peritonitis, a novel murine model of abdominal sepsis. Infect. Immun. *66*, 2300–2309.